

Temperature dependence of step density on vicinal Pb(111)

Z. H. Zhang and H. E. Elsayed-Ali*

Department of Electrical and Computer Engineering, Old Dominion University, Norfolk, Virginia 23529

(Received 9 August 1996; revised manuscript received 27 May 1997)

The temperature dependence of step density on the vicinal Pb(111) surface is investigated using reflection high-energy electron diffraction. When the temperature is increased from 323 to 590 K, the average terrace width and the average string length at the step edge decrease from 85 ± 25 to 37 ± 16 Å and from 220 ± 33 to 25 ± 8 Å, respectively. Thermal step collapse on the Pb(111) surface near its bulk melting temperature is not observed. Above 530 ± 7 K, the change in the string length at the step edge with temperature becomes small, and the intensity of the (00) beam is significantly decreased. We conclude that partial step melting at the step edge occurs at the surface above 530 ± 7 K. [S0163-1829(98)04824-3]

I. INTRODUCTION

It is energetically favorable for some surfaces to disorder at temperatures below the bulk melting point T_m .¹ This phenomenon is called surface disordering.² The general observed trend is that close-packed surfaces remain ordered up to T_m , while open surfaces undergo surface melting. While the top atomic layer of Pb(110) disorders at a temperature as low as 150 K below T_m and undergoes a surface melting transition at $T_m - 40$ K, the Pb(111) surface remains ordered up to $T_m = 600.7$ K.^{2,3} This was confirmed by medium-energy ion scattering experiments on Pb(111) and its vicinal surfaces.³ A cylindrically shaped Pb crystal, exposing many facets, was used to study the dependence of surface premelting on surface orientation. Above 580 K, the (332) and (112) surfaces rapidly disorder with a temperature increase. In contrast, the (111) surface remains ordered up to $T_m - 0.05$ K. For lead microcrystallites bounded by {111} facets, which was grown on graphite, no premelting was observed using scanning electron microscopy (SEM).^{4,5} For a single Pb{111} bounded microcrystallite, a bright ring surrounding the Pb{111} facet was observed above 580 K. This bright ring was also observed to shrink with temperature increase and disappears at T_m .⁴ In another SEM study, Heyraud and Métois measured the surface free-energy anisotropy both above and below the surface melting temperature.⁵ The measured surface energy anisotropy, $\gamma_{(hkl)}/\gamma_{(111)}$, which is the ratio of the free energies of the two faces, decreases as the temperature increases. However, without any surface phase transformation this anisotropy should increase with temperature, because entropy is positive.

In a recent theoretical study, Stewart predicted that, for Pb(111), step melting at the edge occurs below the bulk melting point T_m , whereas the step terrace maintains order up to T_m .⁶ Step melting refers to local melting at a step edge. This model offered an explanation for the results of Pavlovskaya, Faulian, and Bauer in which a ring was observed above 580 K in their SEM study.⁴ In Stewart's model, an isolated step edge on Pb(111) melts locally above 548 K.⁶ The key to step-edge melting is sufficient localization of energy, which means the energy at a step edge may be locally higher than other places at the surface. Energy localization at a step edge forces local melting. Therefore, step melting at

the edge and the difference in secondary electron yield between the solid and the melt causes the observed ring at 580 K. The increase in the liquid thickness at the edge with temperature causes the ring to shrink. Near T_m , the liquid becomes thick and the ring disappears. On the other hand, Stewart's calculations show that vacancy or adatom melting can explain the anomalous behavior of the free-energy anisotropy observed by Heyraud and Métois where the free-energy anisotropy decreases with temperature.⁵ Vacancies and adatoms have a higher localization of energy than steps and are easier to premelt. Both the step and the vacancy melting models offer an explanation for the temperature dependence of Pb{111} microcrystallite shape change and the surface free-energy anisotropy observed in SEM studies. However, except for the experiments on Pb{111} microcrystallites on graphite, few experimental studies on Pb(111) have been carried out to test for step melting, as predicted in Stewart's calculations.

Using high-resolution low-energy electron diffraction (HRLEED), thermal step collapse, i.e., a sudden increase in terrace size, on the single-crystal Pb(111) surface was observed above 580 K.⁷ The average terrace width decreased from 63 Å at room temperature to 34 Å at 573 K, and then became larger than 63 Å above 580 K. Recently, we investigated surface step density after laser superheating of Pb(111) using reflection high-energy electron diffraction (RHEED).⁸ Superheating of Pb(111) by ~ 180 ps laser pulses was observed up to 120 K above T_m in time-resolved RHEED experiments.⁹ In our superheating experiments, Pb(111) maintained at 573 K was heated by ~ 100 ps laser pulses, measured at full-width at half maximum (FWHM). An increase in terrace size is observed when the laser fluence is high enough to cause surface melting after superheating. No detectable collapse of steps below the laser surface melting threshold was observed. These results lead us to consider whether step collapse on Pb(111) occurs below the melting point.

We report on a temperature dependent RHEED study of the surface step density on Pb(111). We investigate the temperature dependence of the average terrace width and the average string length. The terrace width refers to the length of a step terrace, while the string length refers to any line of atoms before an up or down step occurs at the edge.¹⁰ Our

measurements show that the average terrace width and string length at the step-edge decrease with temperature. We did not observe any thermal step collapse on the Pb(111) surface up to the highest temperature studied, 590 K. Above 525 \pm 15 K, the change in the string length at the step edge with temperature becomes small. Above 530 K, we also observed that the (00) beam intensity significantly decreases, consistent with step-edge melting as suggested by the theoretical model of Stewart.⁶

II. EXPERIMENTAL METHODS

An ultrahigh vacuum chamber equipped with RHEED and Auger systems was used. The residual gas pressure in the chamber was less than 7×10^{-11} Torr. The electron beam energy for RHEED was 9 keV. A single-pass cylindrical-mirror electron energy analyzer for Auger was used to check for surface impurity. A 6.4-mm-diam, 2-mm-thick Pb(111) single crystal with 99.999% purity was used. The surface was chemically polished and sputtered clean at 520 K using an argon-ion beam with 1.5–2 keV energy. After sputtering and annealing the sample at 500 K for more than 10 h, the Auger spectrum did not show any detectable impurity, and we obtained a sharp 1×1 RHEED pattern of the Pb(111) surface. The temperature was measured by two thermocouples clipped onto the crystal surface. The thermocouples were calibrated to the bulk melting temperature of Pb, and the boiling point of distilled water. A temperature uncertainty of ± 2 K near the Pb melting point and ± 1 K near the boiling point of water is estimated. Temperature stability within ± 0.1 K was attained using a temperature controller. The RHEED peak intensity and the FWHM of the beam profile were measured using a charge-coupled two-dimensional array detector.

III. RESULTS AND DISCUSSION

Figures 1(a) and 1(b) show the measured RHEED rocking curves for the (00) beam (specular beam) of the clean Pb(111)- 1×1 surface obtained at room temperature with the electron beam incident along the [110] and [112] directions. The RHEED pattern shown in the insert of Fig. 1(b) demonstrates the 1×1 structure of the clean Pb(111) surface, taken with the electron beam incident along the [112] direction, at an incident angle of 3.5° , corresponding to the in-phase condition (Bragg reflection condition). In the pattern, the (00), (11), and $(\bar{1}\bar{1})$ beams are clearly seen. The x - y axis directions indicated below the pattern are the RHEED image line-scan directions used for reference in later discussions of the RHEED intensity analysis of the (00) beam. The arrows show a kinematics calculation of the angles for incidences at the in-phase conditions for Pb(111). A plane distance of 2.86 Å and an inner potential of 14.9 eV were used in the calculation.¹¹ In Fig. 1(a), three peaks indicated by the letters A, B, and C are present. Peaks A and B correspond to the in-phase condition for $n=2$ and 3, respectively. The experimentally observed angles of maximum reflection, 2.0° and 3.5° , are larger than the calculated angles of 1.1° and 3.1° (indicated by arrows) due to the contraction of the top layers at the surface. For calculating such contraction, dynamic calculations are necessary.^{12,13} This contraction of the top layers

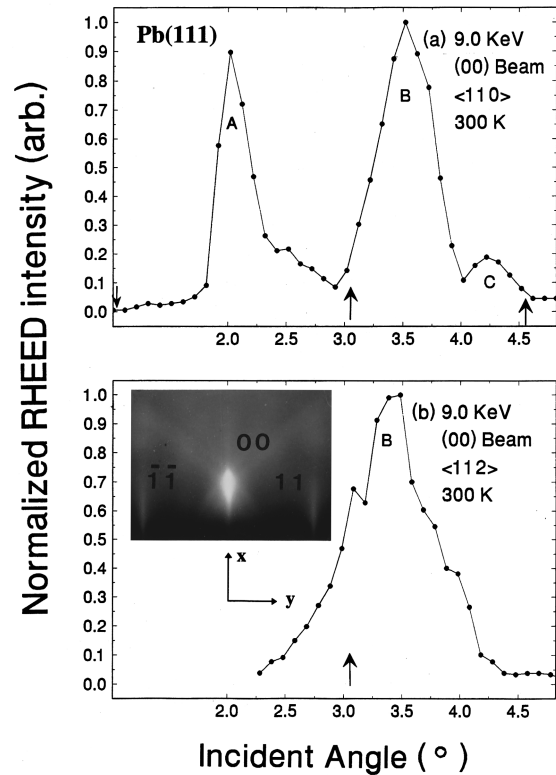


FIG. 1. RHEED rocking curves of the (00) beam for the clean Pb(111)- 1×1 surface obtained at room temperature. The arrows show the calculated angles of incidence at the Bragg reflection condition for Pb(111) with a bulk lattice constant of 2.86 Å. (a) The electron beam is incident along [110] direction; (b) along the [112] direction. The inset shows an RHEED pattern of the Pb(111)- 1×1 structure for the electron beam incident along the [112] direction.

is given by $3.5 \pm 1\%$ as obtained from dynamic calculations based on the measured I - V curves of low-energy electron diffraction.¹⁴ In contrast, the angle corresponding to the maximum reflection of peak C is 4.2° , which is smaller than the calculated Bragg reflection angle of 4.6° for $n=4$. Therefore, we conclude that peak C is due to a surface resonance wave.¹² In Fig. 1(b), peak B which corresponds to the Bragg reflection for $n=3$, appears at 3.5° as for peak B in Fig. 1(a). The RHEED pattern shown in Fig. 1(b) is taken at an incident angle of 3.5° , corresponding to the position of the peak B. In this experiment, the angle of incidence of the electron beam was set between peak B and C, corresponding to the out-of-phase condition.

The sample was heated from room temperature to near T_m . The angle of incidence of the electron beam was set at $\sim 4.1^\circ$, corresponding to the out-of-phase condition. The intensity of the (00) beam was measured at different temperatures. Figures 2(a) and 2(b) show the RHEED intensity profiles of the (00) beam at different temperatures with the electron beam incident along the [110] direction. The profiles are taken parallel and perpendicular to the electron beam, incident along the [110] direction. As shown in Fig. 1(b), the profiles are obtained from the RHEED image line scans through the (00) beam along the x and y directions. In Figs. 2(a) and 2(b), S_x and S_y are the components of the momentum transfer along the x and y directions, where x and y are

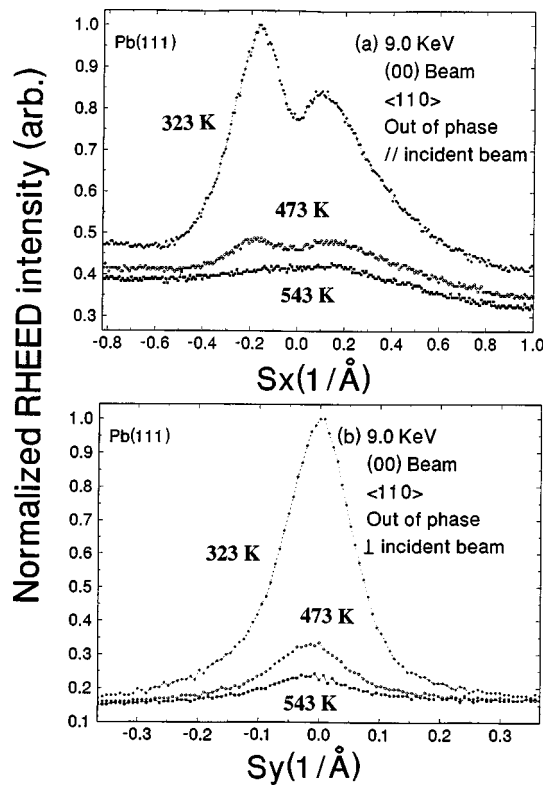


FIG. 2. RHEED intensity profiles of the (00) beam incident along [110] direction at different temperatures. (a) For profiles taken parallel to the [110] direction, a split in the (00) beam producing two peaks along the [110] direction is observed. (b) Profiles taken perpendicular to the [110] direction.

parallel and perpendicular to the direction of the incident electron beam, respectively. In Fig. 2(a), a splitting in the (00) beam, producing two peaks along the [110] direction is observed. This indicates that the surface steps are vicinal and perpendicular to the electron beam incident direction, e.g., the [110] direction.^{10,15} With temperature increase, the two split peaks decrease in intensity and disappear at 543 K, as shown in Fig. 2(a), and the (00) beam profile becomes Lorentzian. This is due to the increase in step randomness and the Debye-Waller factor by which the peak height is decreased. The intensity profiles are asymmetric in Fig. 2(a), which is due to the influence of the background intensity from the shadow edge of the pattern. In Fig. 2(b), a Lorentzian intensity profile is observed and the intensity decreases with temperature. We use the FWHM of the Lorentzian profile in Fig. 2(b) to estimate the average string length on surface step edges.

The intensity profile parallel to the electron beam incident along the [110] direction was analyzed. With temperature increase, the intensity of the split peaks is reduced and the two peaks disappear at 543 K. We measured the changes in the spacing between the two split peaks. Above 543 K, the FWHM of the profile was obtained by fitting it to a Lorentzian. At 323 K, the spacing between the two split peaks is 0.246 \AA^{-1} . The FWHM of the Lorentzian profile, which develops at 543 K, is 0.337 \AA^{-1} and increases to 0.342 \AA^{-1} at 590 K. An instrumental response of 0.172 \AA^{-1} is determined from the FWHM of the (00) beam at the in-phase condition.¹⁶⁻¹⁸ The average terrace width on Pb(111) as a

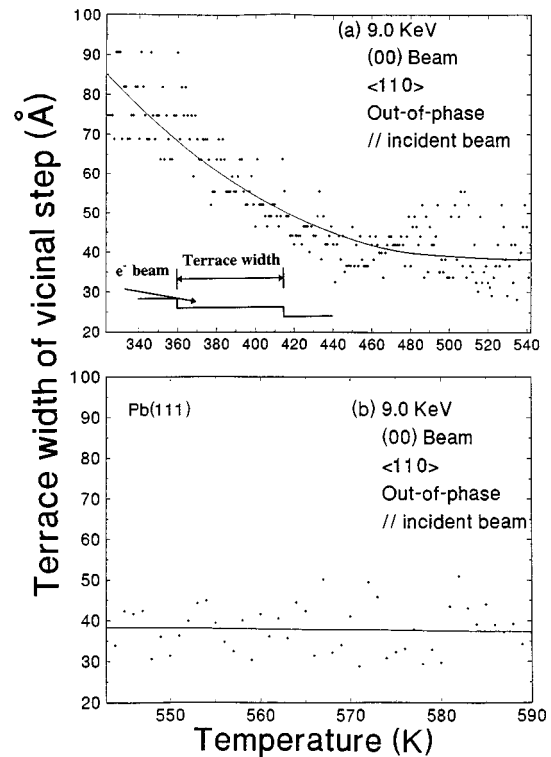


FIG. 3. The terrace width as a function of temperature obtained from intensity profiles parallel to the [110] direction. (a) Terrace width obtained from the changes in the spacing between the two split peaks along the [110] direction below 543 K. (b) Terrace width obtained from the FWHM changes by fitting the (00) beam intensity above 543 K to a Lorentzian profile above 543 K. The terrace width decreases from $85 \pm 25 \text{ \AA}$ at 323 K to $37 \pm 6 \text{ \AA}$ at 590 K. The inset gives a sketch of the terrace width and the electron-beam incident direction.

function of temperature is shown in Figs. 3(a) and 3(b). The insert in Fig. 3(a) shows a sketch of the terrace width and the electron beam incident direction. Figures 3(a) and 3(b) are obtained from the measured spacing between the two splitting peaks and the FWHM of the Lorentzian profile. The terrace width decreases from $85 \pm 25 \text{ \AA}$ at 323 K to $37 \pm 6 \text{ \AA}$ at 590 K. We did not observe any collapse of steps up to 590 K. Dynamic effects do not in general cause the splitting of the peak.¹⁹ The two split peaks due to the vicinal steps can be explained well by the kinematic theory.^{10,15} Therefore, we believe that the results in Fig. 3 can be completely attributed to the change in the terrace width. The change in the terrace width for a vicinal stepped surface with temperature, particularly, below 460 K is due to either facet formation^{4,20} or meandering at step edges.¹⁰ Meandering refers to a turning or winding of the step kinks at the edge increasing step edge roughness. In our case, the vicinal stepped surface does not undergo faceting at low temperatures,^{4,20} which causes the change in the average step terrace width. As discussed later, we observed the occurrence of such meandering with increasing temperature. Therefore, we believe that meandering at step edges causes the terraces to become narrower on the average but the step density stays constant.

The RHEED intensity profile taken perpendicular to the electron-beam direction, which was incident along the [110]

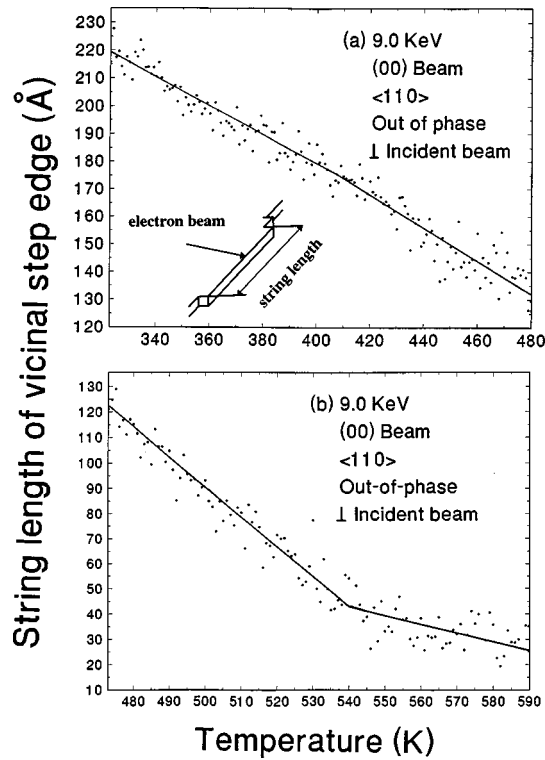


FIG. 4. The average string length at the step edge as a function of temperature obtained from the (00) beam diffraction intensity profiles perpendicular to the [110] direction by fitting to a Lorentzian. (a) 323 K–480 K. (b) 480 K–590 K. The average string length decreases from 220 ± 33 Å at 323 K to 25 ± 5 Å at 590 K. The inset gives a sketch of the string length and the electron-beam incident direction.

direction of the crystal, was also analyzed. Fitting that intensity to a Lorentzian, the FWHM of the (00) profile changes from 0.143 \AA^{-1} at 323 K to 0.365 \AA^{-1} at 590 K. The average string length at the step edge is shown in Figs. 4(a) and 4(b) as a function of temperature, and is observed to decrease from 220 ± 33 Å at 323 K to 25 ± 5 Å at 590 K. The inset shows a sketch of a string length and the electron beam incident direction. In Fig. 4(a), the rate of decrease in the string length is faster near 410 K as evident from the slope change of the line fit, which shows an accelerated increase in surface step roughness. In Fig. 4(b), we observe that the rate of change of the average string length decreases above 540 K, indicating that the increase in step-edge roughening is suppressed at the higher temperatures. Also, from Figs. 4(a) and 4(b) we observed that the rate of change of the average string length decreases near 480 K. Meanwhile, above 540 K the step terrace width in Fig. 3(b) does not significantly decrease. This analysis is based on the kinematic theory. In order to rule out dynamic effects, the (00) spot intensity profile perpendicular to the electron beam which was incident along the [112] direction of the crystal was also analyzed. Dynamic effects are dependent on the azimuthal direction of the electron beam relative to the surface since these effects result from multiple interactions of all diffracted beams.¹⁹ When the electron beam is incident along the [112] direction, the RHEED pattern, in Fig. 1(b), shows the (00), (11), ($\bar{1}\bar{1}$), and high-order streaks. When the electron beam is incident along the [110] direction, the pattern shows the (00), (10),

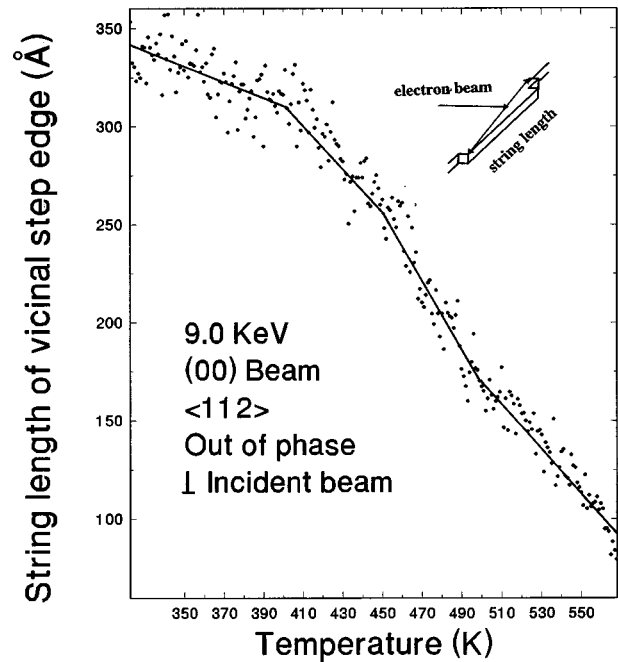


FIG. 5. The average string length at the step edge as a function of temperature obtained from the (00) beam diffraction intensity profiles perpendicular to the [112] direction by fitting to a Lorentzian. The average string length decreases from 340 ± 51 Å at 323 K to 100 ± 20 Å at 570 K. The inset gives a sketch of the string length and the electron-beam incident direction.

($\bar{1}0$), and higher-order streaks. If the observed change in the FWHM of the specular beam with temperature is due to dynamic effects, then these changes will depend on the direction of the incident electron beam. However, we observe that the temperature dependence of the average string length is about the same for the different electron beam directions. For example, the measured average string length at the step edge as a function of temperature measured with the electron beam incident along the [112] direction is observed to decrease from 340 ± 51 Å at 323 K to 100 ± 20 Å at 570 K as shown in Fig. 5. This measured average string length of 340 Å at 323 K is larger than that in Fig. 4(a) which was obtained when the electron beam was incident along the [110] direction. This difference in the absolute value can be explained by considering that when the electron beam is incident along the [112] direction, the angle between the electron beam and the step edge is 60° compared to 90° when the electron beam is incident along the [110] direction, as shown in the inserts in Figs. 4(a) and 5. Therefore, the measured average string length appears larger for the [112] direction. In Fig. 5, as the surface is heated, the rate of decrease in the average string length is increased near 410 and 450 K, then is reduced above ~ 500 K. These measured slope changes are in a good agreement with those in Fig. 4, within the experimental error. The measured average temperature for obtaining the reduced slope is $\sim 525 \pm 15$ K. This agreement in the temperature dependence of the FWHM of the specular beam regardless of the electron-beam direction of incidence indicates that dynamic effects do not affect our measurement of the temperature dependence of the string length. The observed reduced slope above ~ 500 K indicates that temperature-induced step-edge roughening is suppressed.

The change in the measured terrace width due to the step-edge roughening, meandering, is also suppressed above 540 K with temperature increase, as shown in Fig. 3. This leads us to conclude that partial melting occurs at the step edge while the terrace remains ordered, which causes the reduced slope above 530 ± 7 K. In the RHEED pattern taken at 523 K, the (11) and $(\bar{1}\bar{1})$ beams became weaker and the (10) and $(\bar{1}0)$ beams disappeared. At 590 K, we still observe a weak (00) beam in the RHEED pattern. This is well in agreement with Stewart's theoretical calculations which indicated that, above 548 K, an isolated Pb step melts locally with a certain liquid thickness.⁶ Our results also confirm that the observed bright ring above 580 K in the experiment of Pavlovska, Faulian, and Bauer is due to melting at step edges.⁴ Moreover, in the experiments of Plius and co-workers,³ premelting was not observed. However, from the measured ion backscattering energy spectra for Pb(111), an increased number of visible atoms per row above 520 K showed a small deviation from the simulation of the data, which was obtained from the ordered surface. This is probably a result of step-edge melting. Ion scattering is not sensitive to step melting. Diffraction in the out-of-phase condition, as was set in our experiment, is more sensitive to probe the disorder at surface steps.

From Figs. 3, and 4, the measured average terrace width and string length at the step edge do not show a sudden collapse of step density up to 590 K, both the average terrace width and average string length gradually decrease with temperature up to 590 K. In our experiment, we checked repeatedly the uncertainty of the temperature measurement and determined a maximum error of ± 2 K. Bilalbegović, Ercolessi, and Tosatti performed molecular dynamics (MD) simulations of vicinal surfaces of Pb(111).²⁰ The simulation cells were approximately 100 Å long in the direction perpendicular to the steps, and four atoms wide parallel to the steps. At room temperature, the vicinal surface of Pb(111) is a monatomic stepped surface. At $T = 0.97 T_m$, ~ 583 K, the vicinal surface of Pb(111) demonstrates clearly the occurrence of a facet with a flat, crystalline (111) surface, and a tilted, melted surface. Facets with five monatomic steps height and a variety of orientations, which are between 18° and 27° away from the (111) orientation produce a large step terrace. The broadening terrace width is approximately 1.67 times the terrace width of a monatomic step at room temperature, indicating a step collapse. In our experiment, we did not observe such step collapse below 590 K; however, by using laser heating we observed a sudden collapse of steps after laser melting.⁸ This suggests that the temperature for facet formation in our experiments should be higher than 590 K. The theoretically estimated temperature, 583 K in MD simulations, seems to be small.²⁰ In HRLEED experiments, a sudden collapse of steps above 580 K was observed.⁷ Our results cannot be compared directly with the previous HRLEED results due to the different surface morphology. The surface steps at room temperature in HRLEED experiments show randomness in its terrace width or distribution with monatomic height since nonsplitting LEED peaks were observed.⁷ This differs from the vicinal surfaces without randomness in the terrace width observed in our experiments and in the MD simulation.²⁰

Figure 6(a) and 6(b) show the peak intensity changes in

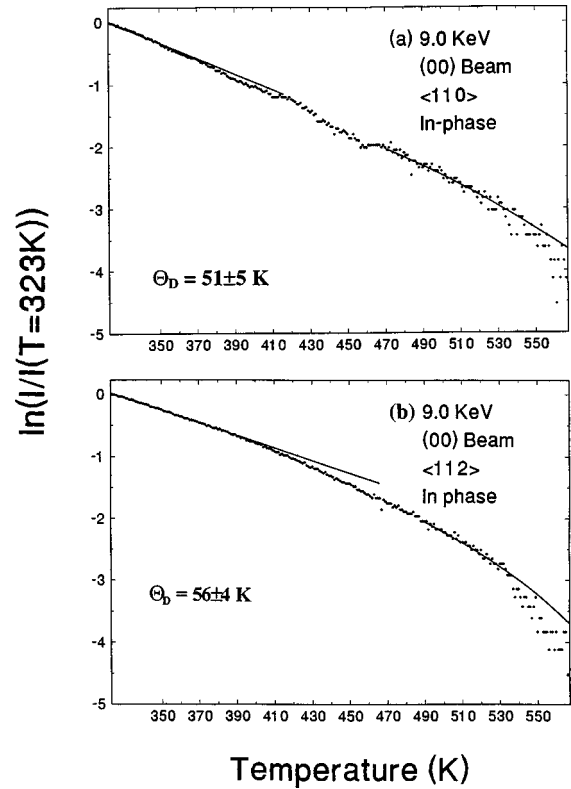


FIG. 6. Peak intensity changes for the (00) beam with temperature at the in-phase condition. The electron beam is incident along the [110] and [112] direction with an angle of incidence of 3.5° . The obtained Debye temperature is 51 ± 5 and 56 ± 5 K, respectively.

the (00) beam with temperature at the in-phase condition taken with the electron beam incident along the [110] and [112] directions. The electron beam angle of incidence was 3.5° . Figures 6(a) and 6(b) show the same changes in the intensity. Below 390 K, the intensity changes linearly with temperature. The Debye-Waller factor is obtained from a least-square fit to these curves between 323 and 390 K. The calculated Debye temperature is 54 ± 5 K. This is the average of the two measured Debye temperatures of 51 ± 4 and 56 ± 4 K from both curves, which show agreement with the previously measured value of 61 ± 7 K.⁹ Both diffraction intensities decrease between 370 and 530 K and deviate gradually from the Debye-Waller dependence, indicating that surface atomic vibrations might become anharmonic. Above 530 K, the intensities decrease dramatically and deviate from the solid line fit. This indicates that surface atomic vibrations might become more anharmonic.

Based on kinematic diffraction, we conclude that these FWHM changes in the RHEED profiles are completely due to changes in the average terrace width and string length, not vacancies.^{8,10,15,21} Without taking into account the instrumental broadening, the RHEED intensity profile from a two-dimensional monatomic stepped surface has a sharp peak, due to the flat surface, and a diffuse intensity in the shape of a Lorentzian function with FWHM depending on step density.^{10,15} For a vicinal stepped surface, the diffuse intensity is more complicated and gives a splitting shape.¹⁵ If the surface is two-dimensional containing only vacancies, an increase in vacancy density increases the background intensity

without broadening the RHEED profile.^{17,21} In our case, FWHM changes were observed, however, we did not observe changes in the background intensity. This was verified by measuring the average background intensities in selected areas in the diffraction pattern as a function of temperature, excluding the reflection spots, and Kikuchi bands and lines. These results indicate that the step melting model applies to high-temperature disorder of Pb(111), and that vacancy melting does not play a key role in the melting of Pb(111).

IV. SUMMARY

In conclusion, for a vertical Pb(111) surface when the temperature is increased from 323 to 590 K, the average terrace width and the average string length at the step edge

decrease from 85 ± 25 to 37 ± 6 Å, and from 220 ± 33 to 25 ± 5 Å, respectively. The surface becomes rough with temperature. Thermal step collapse on the Pb(111) surface is not observed up to 590 K. Above 530 ± 7 K, the change in the average string length at the step edge with temperature becomes small, and the RHEED (00) beam intensity significantly decreases. Our results support the conclusion that partial step melting at the step edge occurs at the surface. The surface Debye temperature is measured to be 54 ± 5 K.

ACKNOWLEDGMENT

This work was supported by the U.S. Department of Energy, under Grant Nos. DE-FG05-93ER45504 and DE-FG02-97ER45625.

*Author to whom correspondence should be addressed. FAX: (757)683-3220. Electronic address: elsayed-ali@ece.odu.edu

¹D. P. Woodruff, *The Solid-Liquid Interface* (Cambridge University Press, London, 1973).

²J. W. M. Frenken and J. F. van der Veen, Phys. Rev. Lett. **54**, 134 (1985); J. W. M. Frenken, P. M. J. Maree, and J. F. van der Veen, Phys. Rev. B **34**, 7506 (1986).

³B. Pluis, A. W. Denier van der Gon, J. W. M. Frenken, and J. F. van der Veen, Phys. Rev. Lett. **59**, 2678 (1987); Phys. Rev. B **49**, 13 798 (1994); B. Pluis, A. W. Denier van der Gon, J. F. van der Veen, and A. J. Riemersma, Surf. Sci. **239**, 265 (1990).

⁴A. Pavlovska, K. Faulian, and E. Bauer, Surf. Sci. **221**, 233 (1989).

⁵J. C. Heyraud and J. J. Métois, Surf. Sci. **128**, 334 (1983).

⁶J. Stewart, Phys. Rev. Lett. **71**, 887 (1993); Phys. Rev. B **49**, 13 826 (1994).

⁷H. N. Yang, T. M. Lu, and G. C. Wang, Phys. Rev. Lett. **62**, 2148 (1989).

⁸Z. H. Zhang, Bo Lin, X. L. Zeng, and H. E. Elsayed-Ali, Phys. Rev. B **57**, 9262 (1998).

⁹J. W. Herman and H. E. Elsayed-Ali, Phys. Rev. Lett. **69**, 1228 (1992).

¹⁰M. G. Lagally, D. E. Savage, and M. C. Tringides, in *Reflection High-Energy Electron Diffraction and Reflection Imaging of Surfaces*, Vol. 188 of *NATO Advanced Studies Institute Series B: Physics*, edited by K. Larson and P. J. Dobson (Plenum, New York, 1988), p. 139.

¹¹M. Jalochowski and E. Bauer, Phys. Rev. B **37**, 8622 (1988); **38**, 5272 (1988).

¹²P. A. Maksym and J. L. Beeby, Surf. Sci. **110**, 423 (1981).

¹³T. Hanada, S. Ino, and H. Daimon, Surf. Sci. **313**, 143 (1994).

¹⁴Y. S. Li, F. Jona, and P. M. Marcus, Phys. Rev. B **43**, 6337 (1991).

¹⁵C. S. Lent and P. I. Cohen, Surf. Sci. **139**, 121 (1984).

¹⁶J. M. Van Hove and P. I. Cohen, J. Vac. Sci. Technol. A **1**, 609 (1983).

¹⁷H. N. Yang, T. M. Lu, and G. C. Wang, Phys. Rev. Lett. **62**, 2148 (1989).

¹⁸T. M. Lu and M. G. Lagally, Surf. Sci. **99**, 695 (1980).

¹⁹M. A. Van Hove and C. M. Chen, *Low Energy Electron Diffraction* (Springer-Verlag, 1989).

²⁰G. Bilalbegović, F. Ercolessi, and E. Tosatti, Europhys. Lett. **17**, 333 (1992).

²¹J. M. Pimbley and T. M. Lu, Surf. Sci. **139**, 360 (1984).